Fission Yeast Mad3p Is Required for Mad2p To Inhibit the Anaphase-Promoting Complex and Localizes to Kinetochores in a Bub1p-, Bub3p-, and Mph1p-Dependent Manner

MOLECULAR AND CELLULAR BIOLOGY, Apr. 2002, p. 2728–2742 Vol. 22, No. 8
0270-7306/02/$04.00+0 DOI: 10.1128/MCB.22.8.2728–2742.2002

Fission Yeast Mad3p Is Required for Mad2p To Inhibit the Anaphase-Promoting Complex and Localizes to Kinetochores in a Bub1p-, Bub3p-, and Mph1p-Dependent Manner

David N. Millband and Kevin G. Hardwick*

Wellcome Trust Centre for Cell Biology, Institute of Cell and Molecular Biology, University of Edinburgh, Edinburgh, Scotland EH9 3JR, United Kingdom

Received 4 October 2001/Returned for modification 19 November 2001/Accepted 17 January 2002

The spindle checkpoint delays the metaphase-to-anaphase transition in response to spindle and kinetochore defects. Genetic screens in budding yeast identified the Mad and Bub proteins as key components of this conserved regulatory pathway. Here we present the fission yeast homologue of Mad3p. Cells devoid of *mad3*$^+$ are unable to arrest their cell cycle in the presence of microtubule defects. Mad3p coimmunoprecipitates Bub3p, Mad2p, and the spindle checkpoint effector Slp1/Cdc20p. We demonstrate that Mad3p function is required for the overexpression of Mad2p to result in a metaphase arrest. Mad1p, Bub1p, and Bub3p are not required for this arrest. Thus, Mad3p appears to have a crucial role in transducing the inhibitory "wait anaphase" signal to the anaphase-promoting complex (APC). Mad3-green fluorescent protein (GFP) is recruited to unattached kinetochores early in mitosis and accumulates there upon prolonged checkpoint activation. For the first time, we have systematically studied the dependency of Mad3/BubR1 protein recruitment to kinetochores. We find Mad3-GFP kinetochore localization to be dependent upon Bub1p, Bub3p, and the Mph1p kinase, but not upon Mad1p or Mad2p. We discuss the implications of these findings in the context of our current understanding of spindle checkpoint function.

The accuracy of chromosome segregation is dependent upon the correct and timely attachment of sister chromatid kinetochores to the microtubules of the mitotic spindle (39). This attachment process must be completed before sister chromatid separation at anaphase can take place. Errors in this process result in an unequal distribution of genetic material to daughter cells and may contribute to tumor progression (9, 34, 37). The Mad2-dependent checkpoint delays sister chromatid separation until each and every kinetochore has achieved bipolar attachment to the mitotic spindle apparatus (for reviews, see references 20, 51, and 43). Sister chromatid separation is regulated by ubiquitin-mediated proteolysis and the spindle checkpoint is able to inhibit sister separation by attenuating the activity of the anaphase-promoting complex (APC), an E3 ubiquitin ligase, that functions to label proteins for destruction by the 26S proteosome (reviewed in reference 60).

Inhibition of APC function occurs principally through inactivation of an accessory factor, called Cdc20p in budding yeast and Slp1p in fission yeast (17, 30, 32, 33). Cdc20p is responsible for the temporal targeting of specific substrates to the APC and is essential for sister separation, becauses it presents the securins Pds1p (*Saccharomyces cerevisiae* [57]), Cut2p (*Schizosaccharomyces pombe* [19]), and PTTG (vertebrates [61]) to the APC. Pds1p functions as an anaphase inhibitor by binding to the protease Esp1p. When bound to Pds1p, Esp1p is prevented from cleaving the cohesin (Scc1p in budding yeast) that holds sister chromatids together. Once Pds1p is destroyed, active Esp1p is released, and sister chromatid separation and spindle elongation ensue (15, 55). Thus, by inhibiting the activity of Cdc20p, the spindle checkpoint prevents sister chromatid separation.

Work with budding yeast originally identified the Mad and Bub proteins as being key components of this important regulatory pathway (29, 35). Since then, work with fission yeast and higher organisms has shown the spindle checkpoint, like many other elements of the cell cycle machinery, to be evolutionarily conserved (22). Mutations in any of the three *MAD* (mitotic arrest deficient) genes, *MAD1* to *-3,* or the three *BUB* (budding uninhibited by benzimidazole) genes, *BUB1* to *-3*, render cells sensitive to microtubule poisons and unable to arrest mitotic progression in response to spindle insult.

Of the known spindle checkpoint components, Mad1p, Mad2p, Mad3p, Bub1p, Bub3p, and Mps1p function in the Mad2p-dependent response to prevent premature separation of sister chromatids. The Mps1 and Bub1 protein kinases are believed to function upstream of the other Mad and Bub proteins (18, 25). Most checkpoint proteins are recruited to unattached kinetochores during the early stages of mitosis in higher eukaryotes (2, 13, 14, 31, 36, 52), and Bub1p does so in fission yeast (7), yet the molecular events that occur once they are at the kinetochore remain largely unknown. Mad1p is a phosphoprotein (24) that is found tightly complexed with Mad2p throughout the cell cycle (12) and is thought to be responsible for targeting Mad2p to unattached kinetochores (13). Similarly Bub3p binds Bub1p and a vertebrate Mad3/Bub1-related protein kinase, BubR1, and may be responsible for targeting these proteins to kinetochores (53).

Changes in the composition of complexes, which may take place at kinetochores, appear to be necessary for spindle checkpoint activation and the consequent delay of sister chro-

* Corresponding author. Mailing address: Wellcome Trust Centre for Cell Biology, Institute of Cell and Molecular Biology, University of Edinburgh, King's Buildings, Mayfield Rd., Edinburgh, Scotland EH9 3JR, United Kingdom. Phone: 44 (0) 131 650 7091. Fax: 44 (0) 131 650 7037. E-mail: hardwick@holyrood.ed.ac.uk.

TABLE 1. Fission yeast strains used in this study

Strain	Genotype	Mating type	Source
DMSP059	Mad3-GFP::*his3*$^+$	h^+	This study
DMSP077	Mad3-GFP::*his3*$^+$ *mad1*Δ::*ura4*$^+$	h^+	This study
DMSP081	Mad3-GFP::*his3*$^+$ *mad2*Δ::*ura4*$^+$	h^-	This study
DMSP104	Mad3-GFP::*his3*$^+$ *bub1*Δ::*ura4*$^+$	h^+	This study
DMSP106	Mad3-GFP::*his3*$^+$ *bub3*Δ::*ura4*$^+$	h^-	This study
DMSP134	Mad3-GFP::*his3*$^+$ *mph1*Δ::*ura4*$^+$	h^+	This study
DMSP074	*mad1*Δ::*ura4*$^+$	h^-	T. Matsumoto
DMSP075	*mad2*Δ::*ura4*$^+$	h^-	T. Matsumoto
DMSP001	*mad3*Δ::*ura4*$^+$	h^-	This study
DMSP037	*bub1*Δ::*ura4*$^+$	h^-	This laboratory
DMSP035	*bub3*Δ::*ura4*$^+$	h^-	This laboratory
KP175	*mph1*Δ::*ura4*$^+$	h^+	S. Sazer
DMSP020	*cut7-24 leu1-32 ade6-210*	h^-	I. Hagan
DMSP048	*mad2*Δ::*ura4*$^+$ *cut7-24*	h^-	This study
DMSP021	*mad3*Δ::*ura4*$^+$ *cut7-24*	h^-	This study
DMSP058	*mad3*Δ::*ura4*$^+$ *nda3KM311*	h^-	This study
DMSP087	*bub1*Δ::*ura4*$^+$ *nda3KM311*	h^-	This study
DMSP088	*nda3KM311*	h^-	This laboratory
DMSP076	Mad3-GFP::*his3*$^+$ *nda3KM311*	h^-	This study
KP136	*lacO*::*lys1 dis1*-GFP-*lacI*(NLS)::*his7 ura4 leu1-32*	h^-	M. Yanagida
DMSP163	*cdc25 lacO*::*lys1 dis1*-GFP-*lacI*(NLS)::*his7 ade6 leu1-32*	h^-	This study
DMSP166	*mad3*Δ::*ura4 cdc25 lacO*::*lys1 dis1*-GFP-*lacI*(NLS)::*his7 ade6 leu1-32*	h^-	This study
Wild type (366)	*ade6-210 leu1-32 ura4D18*	h^-	R. Allshire
Wild type (367)	*ade6-210 leu1-32 ura4D18*	h^+	R. Allshire

matid separation. We have recently demonstrated that during budding yeast mitosis, a Mad1p/Bub1p/Bub3p complex is formed (8). Interestingly Mad3p and Bub2p do not appear to be required for formation of this complex. Bub2p functions in a distinct checkpoint pathway that responds to spindle pole position in budding yeast (see references 20 and 51 for review).

In addition to binding Bub3p, budding yeast Mad3p has the capacity to bind Mad2p and Cdc20p (23), suggesting a function at the effector end of the checkpoint pathway. A related vertebrate protein, the BubR1 protein kinase, has been found associated with $p55^{Cdc20}$ (56) and with the kinesin-related motor CENP-E and APC subunits (1, 10, 11). Two recent reports have highlighted the importance of human BubR1 in in vitro inhibition of the APC (47, 49).

To date, only *mph1*$^+$ (*MPS1*), *bub1*$^+$, and *mad2*$^+$, which are homologous to the Mad2-dependent spindle checkpoint components, have been reported for fission yeast (7, 26, 27, 33). Because it is such a genetically tractable organism with excellent cytology, we set out to complete the lineup by making use of the fission yeast genome sequencing data set. We searched with conserved sequences from the budding yeast genes and uncovered putative *mad3*$^+$ and *bub3*$^+$ homologues. Here we present fission yeast *mad3*$^+$. Our data on *bub3*$^+$ are in preparation and will be presented elsewhere.

We find that *mad3*$^+$ is a nonessential gene under normal growth conditions that functions as part of the Mad2p-dependent fission yeast spindle checkpoint. *mad3*Δ cells show hypersensitivity to microtubule-depolymerizing agents and fail to arrest their cell cycle in response to spindle damage. *mad3*$^+$ shows genetic and biochemical interactions with *mad2*$^+$ and interacts with Slp1p, the spindle checkpoint effector (33), suggesting a terminal role for Mad3p in the checkpoint pathway. In normal mitosis, and upon prolonged spindle checkpoint activation, we find that the Mad3-green fluorescent protein (GFP) construct is recruited to kinetochores that have yet to achieve attachment to spindle microtubules. Finally, we demonstrate that stable recruitment of Mad3-GFP to kinetochores requires the function of Bub1p, Mph1p, and Bub3p, but not that of Mad1p or Mad2p.

MATERIALS AND METHODS

Media, yeast strains, DNA manipulations, and genetic techniques. All strains used in this study are listed in Table 1. Media, transformations, and genetic techniques were essentially as described by Moreno et al. (38) and Allshire et al. (4). YE5S refers to yeast extract medium supplemented with Leu, Ura, Ade, His, and Lys (3). Where required, benomyl (30-mg/ml stock in dimethyl sulfoxide [DMSO]) was added to plates to the final concentration indicated, while 25 μg of Carbendazim (CBZ; Aldrich; 5-mg/ml stock in DMSO) per ml was used to depolymerize microtubules of cells grown in liquid culture (K. E. Sawin, personal communication). YE5SA refers to YE5S plates containing limiting amounts of adenine to allow the development of pink and red colors of *ade6-210* and *ade6-216* colonies. Ch16 minichromosome loss rates were estimated as described previously (16). Briefly, single white colonies were picked from fresh restreaks on YE5SA plates and grown to log phase in YE5S liquid medium. The microtubule-depolymerizing agent CBZ was then added where necessary, and the cultures were incubated for a further 3 h. Cells were collected by centrifugation, diluted in YE5S, and plated on YE5SA plates. Plates were then incubated for 3 days at 32°C. The rate of minichromosome loss per division is recorded as the number of colonies with a red sector covering half of the colony divided by the total number of colonies minus the number of completely red colonies.

Identification and disruption of the *mad3*$^+$ ORF. The putative *mad3*$^+$ open reading frame (ORF) was identified by BLAST searching (5) of the *S. pombe* genome project data set with the *S. cerevisae MAD3* region I DNA sequence (see Fig. 1A for a schematic representation of Mad3p). A *ura4*$^+$-marked *mad3* deletion strain (DMSP001) was constructed with sequence information of the 5′ and 3′ flanks of the putative *mad3*$^+$ ORF and the PCR-based gene-targeting method of Bahler et al. (6) by using primers SPM3KOF (ATTTTCATTTAGT GGAAAGGTATAGGGTTCTCTAGAAAAGGTTTACTAATTTTTTGGA AGACATTGACTACAAATGGCGCCAGGGTTTTCCCAGTCAC) and SPM3KOR (TTCCGGGAGTCATGATGTACAATAGTTGTTAATCTAAT AACGCCAATACTTTAAATCTTTTCTTTATCGGTTATTAGCGGATAA CAATTTCACACA). Correctly targeted gene disruptions were identified by PCR amplification over both the 5′ and 3′ junctions as well as an inability to apply PCR to portions of wild-type *mad3*$^+$.

DNA manipulations. DNA manipulations were performed by standard techniques. Sequencing was carried out with either plasmid DNA or PCR-generated

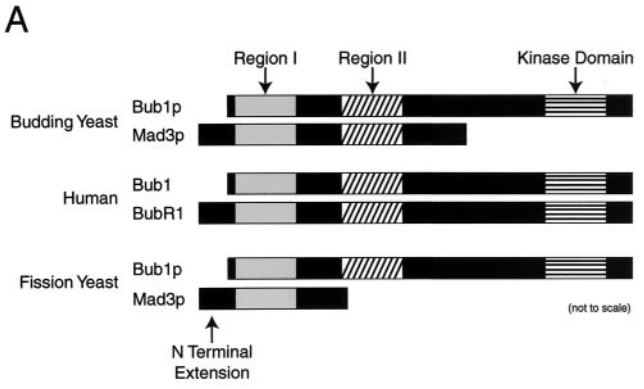

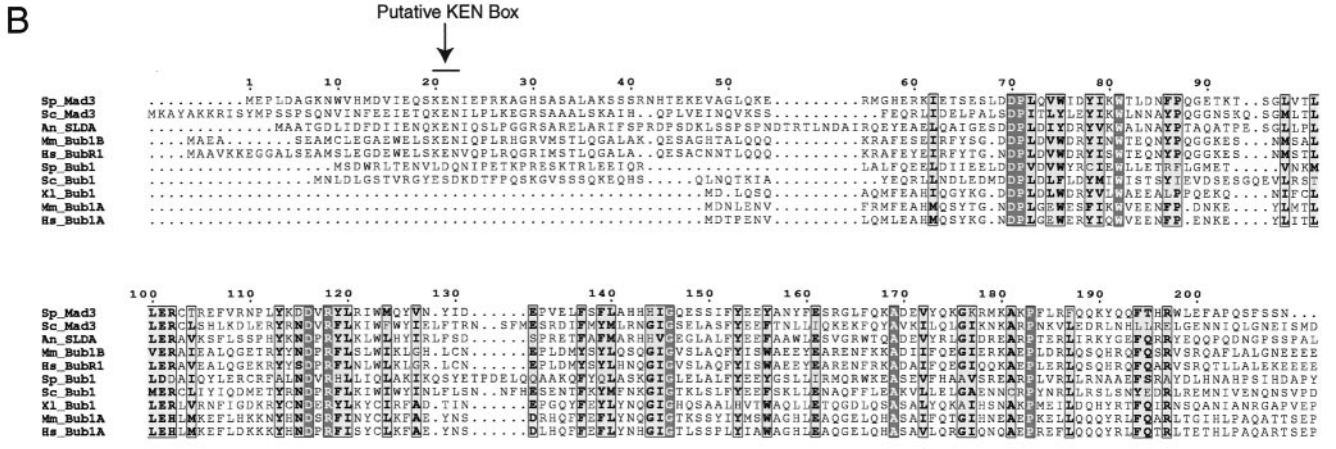

FIG. 1. Identification and disruption of *mad3*$^+$. (A) Schematic comparison of gross Mad3 protein structure. Fission yeast Mad3p (SPCC895.02), like budding yeast Mad3p, is relatively short and lacks a C-terminal kinase domain. (B) ClustalX sequence alignment across region I highlighting the homology shared between Mad3p (SPCC895.02) and other Mad3/Bub1-like proteins. Mad3-like proteins have a short N-terminal extension, containing a putative KEN box motif, compared to Bub1 proteins. Sp, *S. pombe*; Sc, *S. cerevisiae*; An, *Aspergillus nidulans*; Mm, *Mus musculus*; Hs, *Homo sapiens*; *Xl*, *Xenopus laevis*.

double-stranded templates with an Applied Biosystems dRhodamine sequencing kit and an ABI prism 377 sequencer.

Construction of an integrating C-terminal GFP tagging vector. The full-length *his3*$^+$ gene and necessary upstream promoter sequences were cut from pAF1 as a *Bgl*II fragment and subcloned into the *Bam*HI site of pBluescript KS-GFP (GFP in pBluescript as an *Eco*RI-*Bam*HI fragment [this laboratory]) destroying the *Bam*HI site in the process. This manipulation resulted in plasmid pDM084-GFP-*his3*$^+$ and left three unique sites (*Kpn*I, *Apa*I, and *Sal*I) from the pBluescript polylinker 5′ to the ATG of GFP suitable for being cloned into. Cloning with the *Sal*I site, which lies in frame with the GFP ATG start codon, generates a fusion protein with an 11-amino-acid linker (VDGIDKLDIGF) between the cloned ORF and GFP.

Construction of C-terminally tagged Mad3-GFP strains. To make a chromosomally integrated *mad3*$^+$ strain C-terminally tagged with GFP, *mad3*$^+$ was PCR amplified with primers SPMAD3KPNF (CATGGGTACCATGGAACCATTA GATGCGGC) and SPMAD3SALR (CATGGTCGACTTCTTTCGATACTTC CTC) and cloned into the *Kpn*I-*Sal*I sites of plasmid pDM084 (pBluescript *GFP his3*$^+$), resulting in plasmid pDM087 (*mad3*$^+$*-GFP his3*$^+$). pDM087 was then further modified by *Kpn*I-*Bsm*BI digestion to remove 187 bp from the 5′ end of the *mad3*$^+$ ORF, creating plasmid pDM092 (C-terminal *mad3*$^+$*-GFP his3*$^+$). The resultant constructs were sequenced and shown to be in frame with the methionine of GFP and void of mutations. Linear targeting constructs were then prepared prior to electrotransformation into yeast by treating with *Psh*AI, which cuts uniquely within the *mad3*$^+$ insert. Transformation events that resulted in correct targeting to the 3′ end of the *mad3*$^+$ locus were detected by diagnostic PCR amplification over the junction with primers 5′GFPR (GTACATAACCT TCGGGCATGGC) and SPM35′SALGN (TATGTCGACTATGGAACCATT AGATGGC) followed by Western blot analysis. The benomyl sensitivity of this strain is indistinguishable from that of the wild type, indicating that Mad3-GFP is fully functional.

Analysis of cell cycle position by flow cytometry. Propidium iodide staining of cells for DNA content analysis by flow cytometry was carried out as previously described (3). Cells were first pelleted by centrifugation and then fixed by the addition of 70% ethanol. Approximately 2×10^6 to 3×10^6 cells were then rehydrated in 5 ml of 50 mM sodium citrate before being spun at $800\times g$ for 5 min. Cells were then resuspended in 0.5 ml of sodium citrate containing 0.1 mg of RNase A per ml. After a 2-h incubation at 37°C, 0.5 ml of sodium citrate containing 8 mg of propidium iodide per ml was added. Samples were then either stored at 4°C overnight or counted immediately. In all cases, 10,000 cells were counted per sample with a Becton & Dickinson FACSCAN automated counter.

Sister-chromatid separation. We directly visualized premature sister chromatid separation events in *mad3*Δ by using the LacI-GFP/LacO repeat system previously described (50). We constructed strains (DMSP163 and -166) containing GFP-marked chromosome I, along with *cdc25* and *mad3*Δ mutations. These were arrested at 36°C for 4 h and then released by lowering the temperature to 18°C. Duplicate cultures were then grown in the presence of the microtubule poison CBZ (25 μg/ml). At 15-min intervals, samples were taken from the cultures, resuspended in PEM (50 mM PIPES [pH 7.6], 1 mM EGTA, 1 mM $MgSO_4$) plus CBZ, and analyzed for sister chromatid separation. When this occurred, the single GFP spot marking chromosome I became two spots. This

was done with living cells, because we found the GFP signals to be too faint in fixed cells for reliable scoring.

Coimmunoprecipitations. Immunoprecipitations were carried out essentially as previously described (24). The lysis buffer contained the following: 50 mM HEPES (pH 7.6), 75 mM KCl, 1 mM $MgCl_2$, 1 mM EGTA, 0.1% Triton X-100, 1 mM phenylmethylsulfonyl fluoride, LPC (10 μg of leupeptin, pepstatin, and chymostatin per ml), and 1 mM DTT was added after the clarifying spin.

For the immunoprecipitations, we used an anti-GFP mouse monoclonal antibody, 3E6 (Molecular Probes [0.5-mg/ml stock used at 1/100]). To probe the immunoblots, we used a polyclonal rabbit anti-GFP antibody (Molecular Probes [2-mg/ml stock used at 1/1,000 in BLOTTO]). Polyclonal rabbit anti-Mad2p and anti-Slp1p antibodies (kindly provided by T. Matsumoto) were used at a 1/100 dilution.

To immunoprecipitate Bub3-Myc, we used coupled 9E10-Sepharose (Santa Cruz Biotech, Inc.) and to detect the Myc tag on immunoblots, we used either a polyclonal rabbit anti-Myc antibody (A14; Santa Cruz) at 1/1,000 in BLOTTO or the mouse monoclonal antibody 9E10 (Boehringer) at a 1/1,000 dilution in BLOTTO. When immunoblotting, we used horseradish peroxidase-linked secondary antibodies at 1/5,000 (Amersham Pharmacia), followed by enhanced chemiluminescence with the Amersham ECL system.

Visualization of Mad3-GFP and colocalization studies with immunofluorescence. To visualize Mad3-GFP when no costaining for other epitopes was required, mid-log-phase cells grown at 23°C were collected by centrifugation and resuspended in 100% methanol. Cells were then stored in methanol for up to 1 week before analysis. Prior to microscopic analysis, cells were collected by centrifugation and rehydrated in 1× phosphate-buffered saline.

When cells were required for costaining experiments, mid-log-phase cultures were grown in YE5S at 23°C and fixed for 20 min by the addition of freshly prepared paraformaldehyde solution (added to a final concentration of 3.7%, made up as a 10× stock in PEM). Cells were collected by centrifugation and washed three times in PEM (50 mM PIPES [pH 7.6], 1 mM EGTA, 1 mM $MgSO_4$) before being resuspended in 0.5 ml of PEMS (PEM containing 1.2 M sorbitol). To prepare spheroplasts, 0.5 ml of PEMS containing 3 mg of 20T Zymolyase per ml was added prior to incubation at 37°C for 90 min. Spheroplasts were then gently washed three times with PEMS before being left to stand for 1 to 2 min to permeabilize in PEMS containing 1% Triton X-100. Cells were again washed and then blocked in PEMBAL (50 mM PIPES [pH 7.6], 1 mM EGTA, 1 mM $MgS0_4$, 1% bovine serum albumin, 100 mM lysine hydrochloride) for a minimum of 30 min. Incubation in primary antibody was carried out overnight at 4°C, followed by three 5-min washes in PEM before incubation for 4 h in the appropriate secondary antibody. Primary antibodies used in this study were sheep anti-Cnp1/Cenp-A (used at 1/750; kindly provided by B. Mellone and R. Allshire), mouse anti-TAT1 (used at 1/50; a gift from K. Gull), and rabbit anti-GFP (used at 1/10,000; Molecular Probes). All secondary antibodies were Alexa dye coupled and used at 1/500 (Molecular Probes). After incubation with antibody, cells were washed three times for 5 min before being resuspended in PEM. Samples were then mounted upon polylysine-coated slides in Vectashield mounting medium (Vector Laboratories) containing 4′,6′-diamidino-2-phenylindole (DAPI; 1.5 μg/ml). Visualization and image capture were performed with a Zeiss Axioscope fluorescence microscope and either QUIPS-FISH (Vysis) or OpenLab image capture software (Improvision).

RESULTS

Identification of the *mad3*$^+$ gene. Upon BLAST searching of the *S. pombe* genome sequencing project data set with the region I sequence (Fig. 1A and B) of budding yeast *MAD3*, we identified a cosmid (SPCC895) from chromosome III containing a putative *mad3*$^+$ ORF (SPCC895.02 and 059767). *mad3*$^+$ is a 933-bp gene encoding a protein with a predicted molecular mass of 36 kDa. Detailed sequence alignments with ClustalX (54) with budding yeast Mad3p revealed an overall sequence identity of 31%. *mad3*$^+$ is smaller than the budding yeast gene, yet it clearly contains the N-terminal region I domain shown in budding yeast to be important for Cdc20p and Mad2p binding (23). Attempts to align the C-terminal portion of *S. pombe* Mad3p failed to reveal any clear sequence homology with budding yeast Mad3p or Bub1p, or its mammalian relatives, BubR1 and Bub1. Thus, fission yeast Mad3p clearly lacks a C-terminal kinase domain, and it appears from computer alignments that it also lacks homology with budding yeast region II, which was shown to be sufficient for Bub3p binding (23). We confirmed these important observations by sequencing the 3′ end of *mad3*$^+$ from our wild-type strain, 366. Our sequence was identical to that in the Sanger Centre database (data not shown).

ClustalX alignments of the N terminus of yeast and human Mad3 and Bub1 proteins revealed that all the Mad3/BubR1 members have an N-terminal extension, compared to Bub1, and that this contains a sequence resembling a KEN box (Fig. 1B). Such a KEN box was originally defined as a recognition signal sufficient for Cdh1-APC-dependent proteolysis (40). This is an intriguing observation, suggesting that abundance of Mad3p and BubR1 may be regulated at the level of proteolysis.

Fission yeast *mad3*$^+$ is an essential component of the spindle checkpoint. A *mad3*$^-$ null allele was made by replacing the full length of the putative *mad3*$^+$ ORF with the *ura4*$^+$ gene (see Materials and Methods for details). Correct gene targeting was confirmed by PCR analysis of the junctions of the recombination event. The resultant haploid strains were viable, showing that *mad3*$^+$ is not an essential gene in fission yeast. In budding yeast, *mad3*Δ strains are also viable, but show sensitivity to microtubule-depolymerizing agents, such as benomyl and nocodazole, as a consequence of their loss of spindle checkpoint function (35) (23). Spotting serial dilutions of *S. pombe mad3*Δ cells onto YE5S plates containing the microtubule poison benomyl showed that they are unable to form colonies on medium containing 7.5 μg of benomyl per ml (Fig. 2A).

To determine whether *mad3*Δ cells were sensitive to spindle defects of another kind, we crossed the *mad3*Δ gene into a *nda3KM311* background. At 16°C, *nda3KM311* cells fail to form a mitotic spindle, due to a cold-sensitive mutation in β-tubulin, and arrest their cell cycle via the spindle checkpoint prior to the metaphase-anaphase transition. They remain viable for several hours and are able to form colonies when returned to the permissive temperature (26, 28). We asked whether *mad3*Δ *nda3KM311* double mutants retain viability following spindle disruption. After 6 h of incubation at a restrictive temperature of 16°C, the single mutants (*mad3*Δ or *nda3KM311*) maintained high viability (>95%), while the double mutant strain (*mad3*Δ *nda3KM311*) had a much reduced viability (~45%) (Fig. 2B). This behavior was essentially identical to that of an *nda3KM311* strain carrying a *bub1* deletion. The *mad3*Δ *nda3KM311* cells died rapidly at the nonpermissive temperature as a consequence of a failure to recognize that their spindle structure has been compromised. DAPI and calcofluor staining (Fig. 2B) revealed many cells with a *cut* phenotype in the double mutant cultures, indicative of cell cycle progression in the absence of successful chromosome segregation. This result is consistent with the five- to sevenfold-elevated minichromosome (Ch16) loss rates that we observe in *mad3*Δ cells when they are challenged with microtubule poisons (data not shown).

Next we wished to know if *mad3*Δ cells exit mitosis and reenter the next round of cell division when their spindle structure is compromised. To test this, we constructed a *mad3*Δ *cut7* double mutant. *cut7*$^+$ encodes a kinesin-related microtubule motor protein that is essential for interdigitating microtubules

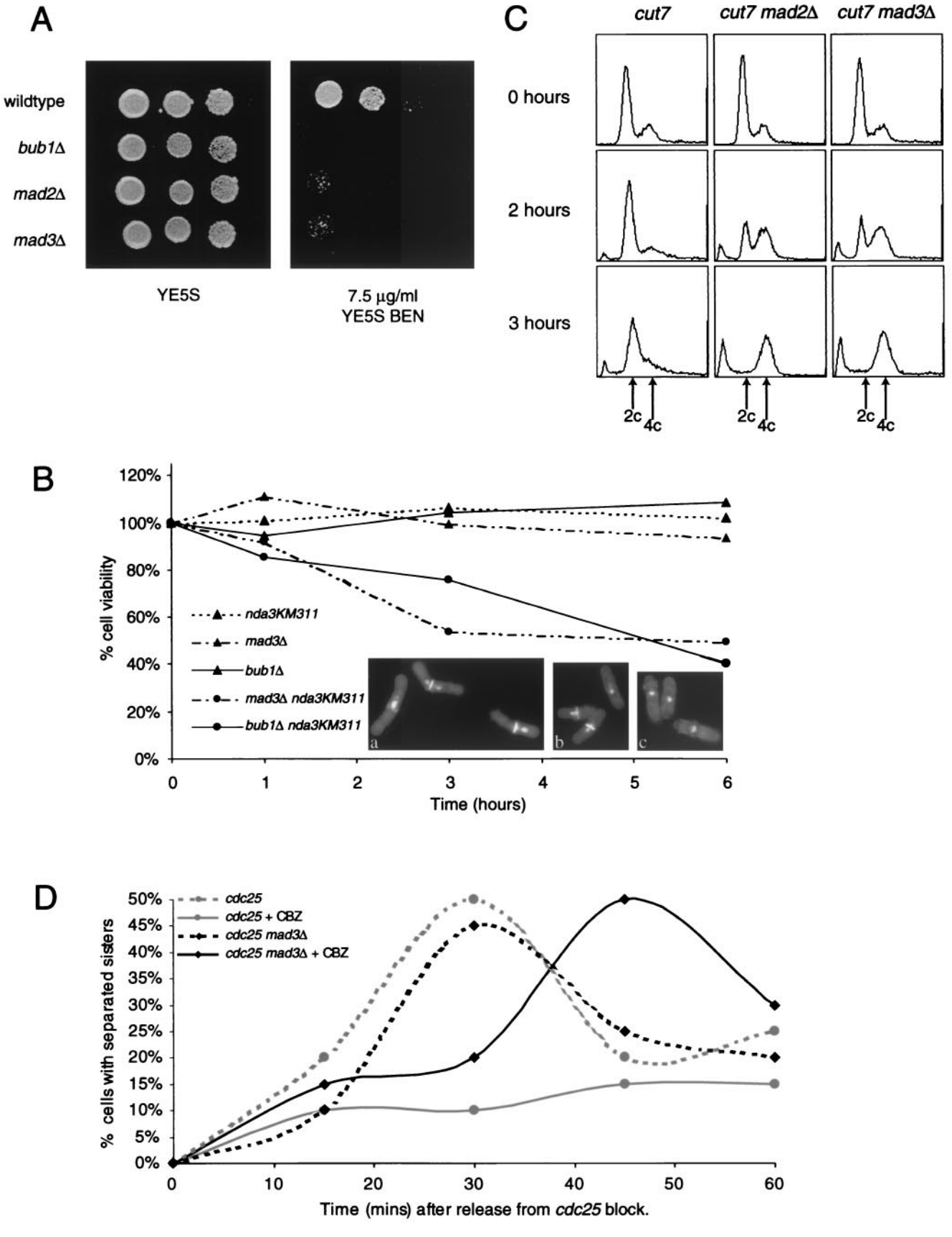
A
wildtype
bub1Δ
mad2Δ
mad3Δ
YE5S
7.5 µg/ml
YE5S BEN
C
cut7
cut7 mad2Δ
cut7 mad3Δ
0 hours
2 hours
3 hours
2c
4c
B
% cell viability
Time (hours)
nda3KM311
mad3Δ
bub1Δ
mad3Δ nda3KM311
bub1Δ nda3KM311
a
b
c
D
% cells with separated sisters
Time (mins) after release from cdc25 block.
cdc25
cdc25 + CBZ
cdc25 mad3Δ
cdc25 mad3Δ + CBZ

of the two half spindles (21). *cut7–24* mutants fail to form a functional spindle and arrest as septated cells, with overcondensed chromosomes suggesting that the loss of *cut7*$^+$ function is ordinarily recognized by the spindle checkpoint. We reasoned that deletion of *mad3*$^+$ might prevent the arrest in the *cut7* mutant, because work previously described for the spindle checkpoint component *mad2*$^+$ (33) had shown the arrest to be checkpoint dependent. Log-phase populations of *cut7–24*, *mad2*Δ *cut7–24* and *mad3*Δ *cut7–24* cells were grown and then shifted to the restrictive temperature of 37°C for various times, after which the DNA content, and thus cell cycle position of the culture, was ascertained by flow cytometry. Figure 2C clearly shows that after 2 h at the restrictive temperature, the *mad3*Δ *cut7–24* cells (like the positive control *mad2*Δ *cut7–24* cells) had rereplicated their genetic material, as evidenced by a 4C peak in the fluorescence-activated cell sorting (FACS) profile. In contrast, at the same time point, the *cut7* single mutant showed a strong 2C peak with little evidence of rereplication, indicative of a mitotic arrest. After 3 h, the entire *mad3*Δ *cut7–24* population had rereplicated, forming 4C and aploid peaks. Thus, at the restrictive temperature, when spindle assembly is compromised, *mad3*Δ *cut7–24* double mutants erroneously exit mitosis and enter the next round of DNA replication.

In addition, we directly visualized premature sister chromatid separation events in *mad3*Δ by using the LacI-GFP/LacO repeat system previously described (50). The *cdc25* and *cdc25 mad3*Δ strains (DMSP163 and -166), both containing GFP marked chromosome I, were arrested at 36°C for 4 h and then released from this G_2 arrest by lowering the temperature to 18°C. Half of the cells were then grown in the presence of the microtubule poison CBZ. At 15-min intervals, samples were taken from the cultures and analyzed for sister chromatid separation—when this occurred, the single GFP spot marking chromosome I became two spots. Figure 2D demonstrates that the two strains separated their sisters with the same kinetics under normal conditions (dashed lines). However, in the presence of CBZ, the *mad3*Δ strain separated its sisters around 45 min after the release from G_2, while the control strain was able to maintain a mitotic arrest and sister chromatid cohesion.

We conclude from the four independent criteria—increased sensitivity to microtubule-depolymerizing agents, an inability to maintain viability after cold treatment in an *nda3KM311* background, DNA rereplication in the absence of a functional mitotic spindle, and the precocious separation of sister chromatids—that fission yeast *mad3*$^+$ function is essential for spindle checkpoint function.

Mad3p is required for overexpressed Mad2p to arrest the cell cycle. Having established a checkpoint role for *mad3*$^+$, we wished to investigate how it might interact with other spindle checkpoint components. Overexpression of *mad2*$^+$ in an otherwise wild-type background results in a metaphase arrest (26). We asked whether such a metaphase arrest is dependent upon *mad3*$^+$ by comparing the *mad2*$^+$ overexpression phenotype in wild-type, *mad3*Δ, and other checkpoint-defective cells. *mad2*$^+$ overexpression (pREP3x-*mad2*$^+$, from which Mad2p is overexpressed in the absence of thiamine) in most checkpoint-defective cells (*mad1*Δ, *bub1*Δ, and *bub3*Δ) gave a mitotic arrest essentially as seen in the wild type, suggesting that those proteins function upstream of Mad2p. The notable exception to this was the *mad3*Δ mutant, which showed no effect upon *mad2*$^+$ overexpression (Fig. 3A). We next performed an anti-Mad2p Western blot, to demonstrate that this was not due to an effect of the *mad3* mutation on the expression level or stability of Mad2p. Whole-cell extracts were prepared from wild-type and checkpoint mutant strains that had been induced to overexpress Mad2p from an *nmt* promoter through the absence of thiamine. These extracts were then separated by sodium dodecyl sulfate-polyacrylamide gel electrophoresis (SDS-PAGE) and immunoblotted with anti-Mad2p antibodies (Fig. 3B). All strains, including *mad3*Δ, overexpressed Mad2p to a similar extent from pREP3x. In addition, we quantitated the numbers of short spindles observed in the cultures overexpressing Mad2p (Fig. 3C). While ~70% of the cells in wild-type, *mad1*Δ, *bub1*Δ, and *bub3*Δ cultures overexpressing Mad2p contained cells with short spindles, indicative of a Mad2p-induced metaphase arrest, only 8% of *mad3*Δ cells contained short spindles, as determined by antitubulin immunofluorescence. This demonstrates that Mad2p overexpression leads to a metaphase arrest, as previously reported for wild-type cells (26), even in the absence of the Bub1p, Bub3p, and Mad1p checkpoint proteins. However, the *mad3* mutant strain

FIG. 2. *mad3*Δ cells are spindle checkpoint defective. (A) *mad3*Δ cells are hypersensitive to microtubule poisons. Fission yeast cells (366, DMSP037, DMSP075, and DMSP001) were spotted in serial dilutions onto YE5S plates containing the indicated concentrations of benomyl and were photographed after 3 days of growth at 30°C. (B) *mad3*Δ cells fail to arrest their cell cycle and rereplicate their DNA when their spindle structure is perturbed. The results of flow cytometric analysis of DNA content of *cut7*-24 (DMSP020), *mad3*Δ *cut7*-24 (DMSP021) and *mad2*Δ *cut7*-24 (DMSP048) cells after incubation at 37°C for the indicated time periods are shown. Cell number is plotted on the *y* axis, and DNA content (relative fluorescence) is on the *x* axis. Arrows indicate the relative fluorescence corresponding to 2C and 4C DNA content (peaks were assigned by using nitrogen-starved, wild-type haploid and diploid log-phase cultures as reference populations [data not shown]). (C) *mad3*Δ cells die rapidly when their spindle structure is compromised. The indicated strains (DMSP001, DMSP037, DMSP058, DMSP087, and DMSP088) were grown to log phase in liquid YE5S medium at the permissive temperature (30°C) before being shifted to the restrictive temperature (16°C). At 0, 1, 3, and 6 h after the temperature shift, samples were taken, plated on YE5S plates, and incubated at the permissive temperature. Colonies on each plate were counted, and cell viability was calculated relative to the time zero samples. DAPI and calcofluor staining (6-h time point shown) revealed many cells with a *cut* phenotype in the double mutant *bub1*Δ *nda3KM311* (DMSP088) (a) and *mad3*Δ *nda3KM311* (DMSP058) (b) cultures, while the single mutant *nda3KM311* (DMSP087) (c) culture remained tightly arrested. (D) Sister chromatids separate prematurely in *mad3*Δ cells treated with microtubule poisons. *cdc25* (DMSP163) and *cdc25 mad3*Δ (DMSP166) strains, both containing GFP-marked chromosome I, were arrested at 36°C for 4 h and then released from this G_2 arrest by lowering the temperature to 18°C. Half of the cells were then grown in the presence of the microtubule poison CBZ. At 15-min intervals, samples were taken from the cultures and analyzed for sister chromatid separation—when this occurred, the single GFP spot marking chromosome I became two spots. The two strains separated their sisters with the same kinetics under normal conditions (dashed lines). However, in the presence of CBZ, the *mad3*Δ strain separated its sisters around 45 min after the release from G_2, while the control strain was able to maintain a mitotic arrest and sister chromatid cohesion (solid lines).

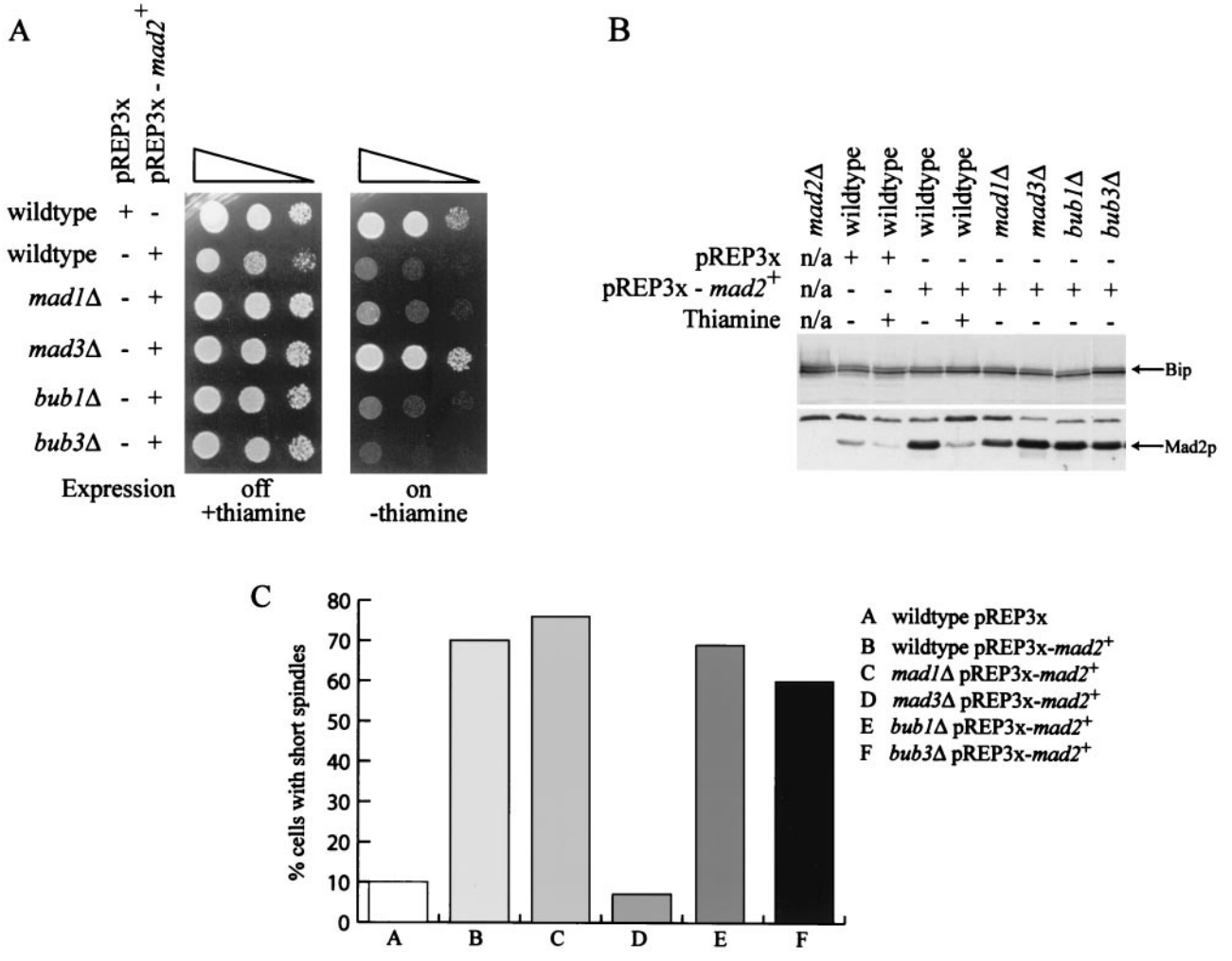

FIG. 3. Mad3p functions at the effector end of the spindle checkpoint pathway. (A) Mad3p is required for the effects of *mad2*$^+$ overexpression. Wild-type cells (366 strain) and spindle checkpoint mutants (*mad1*Δ [DMSP074], *mad3*Δ [DMSP001], *bub1*Δ [DMSP037], and *bub3*Δ [DMSP035]) were transformed with pREP3X-*mad2*$^+$. Transformants were then spotted onto EMM plates with and without the addition of thiamine. Plates were photographed after 3 days of growth at 30°C. (B) Mad2p protein levels are not affected by the *mad3* deletion. Wild-type and checkpoint mutant strains were grown as indicated (± pREP3x-*mad2*$^+$, ± thiamine), and whole-cell extracts were prepared and separated by SDS-PAGE. Immunoblots were carried out with polyclonal anti-Mad2p antibodies and anti-BiP antibodies as a loading control. Mad2p levels were induced in all strains containing pREP3x-*mad2*+ in the absence of thiamine. (C) Mad2p-induced metaphase arrest is Mad3p dependent. Cultures of the strains indicated were fixed and stained for the presence of mitotic spindles with antitubulin antibodies. Only the *mad3*Δ culture failed to accumulate short spindles when Mad2p was overexpressed.

showed no such arrest upon Mad2p overexpression. This striking result demonstrates that *mad3*$^+$ function is required for *mad2*$^+$ overexpression to mediate a checkpoint arrest and therefore that Mad3p functions at the effector end of the checkpoint pathway, downstream of most checkpoint components.

Mad3p coimmunoprecipitates Mad2p, Slp1p, and Bub3p. Our genetic and sequence analysis of *mad3*$^+$ prompted us to ask whether Mad3p physically interacts with other components of the spindle checkpoint pathway. We have previously presented immunoprecipitation and two-hybrid data from budding yeast in support of biologically relevant interactions between Mad3p and Mad2p, Bub3p, and Cdc20p (23). We wished to determine if this held true in fission yeast. To test such interactions, we constructed strains containing a C-terminal GFP tag on Mad3p and a C-terminal 13×Myc tag on Bub3p. These constructs were integrated into the genome at the *mad3*$^+$ and *bub3*$^+$ loci and are driven from their native promoters. Coimmunoprecipitation experiments were then carried out.

To test for an interaction between Mad3p, Mad2p, and Slp1p, we immunoprecipitated Mad3-GFP from cells with and without checkpoint activation (by using the *nda3KM311* mutant or CBZ treatment) with a mouse monoclonal anti-GFP antibody and then blotted with the appropriate anti-GFP, anti-Mad2p, or anti-Slp1p polyclonal antibodies. We found that both Mad2p and Slp1p coimmunoprecipitated with Mad3-GFP from cells that had been arrested at metaphase with their spindle checkpoint active (Fig. 4A). These results strongly support the idea that Mad3p functions downstream in the check-

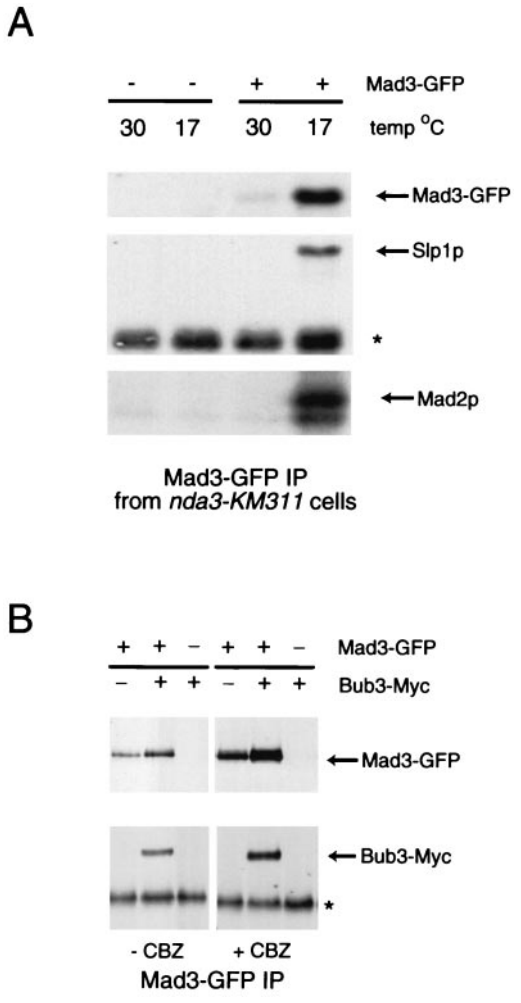

FIG. 4. Mad3p coimmunoprecipitates with Bub3p, Mad2p, and the spindle checkpoint effector, Slp1/Cdc20p. (A) Mad3p interacts with Mad2p and the Cdc20p homologue Slp1p in checkpoint-arrested cells. Mad3-GFP was immunoprecipitated from *nda3KM311* cells, which had been grown either to mid-log phase at 30°C or to mid-log phase at 30°C and then arrested at the metaphase-to-anaphase transition by incubation for 6 h at the restrictive temperature of 17°C. The immunoprecipitates were then separated by SDS-PAGE and immunoblotted with antibodies specific for GFP, Slp1p, and Mad2p. (B) Mad3p interacts with Bub3p. Mad3-GFP was immunoprecipitated from strains containing Bub3-Myc. Cells were grown both in the absence and in the presence of CBZ (3 h at 23°C) to activate the spindle checkpoint. The GFP immunoprecipitates were separated by SDS-PAGE and immunoblotted with antibodies specific for GFP and Myc. Asterisks indicate immunoglobulin heavy chains from the immunoprecipitations.

point pathway, in that it stably interacts with both Mad2p and the spindle checkpoint effector, Slp1p.

Computer analysis failed to align the C terminus of fission yeast Mad3p with region II of the budding yeast Mad3p or its vertebrate BubRI homologues. Because this region is sufficient for Bub3p binding (23), we wanted to test for a Mad3p-Bub3p interaction in *S. pombe*. Figure 4B shows that when Mad3-GFP was immunoprecipitated from strains containing Bub3-Myc, that protein was coimmunoprecipitated. This interaction doesn't require checkpoint activation, because the two proteins interacted even in the absence of CBZ. Thus, a constitutive Mad3p-Bub3p interaction has been conserved in fission yeast.

Mad3-GFP localization during unperturbed mitosis. To date, Mad3p has simply been shown to localize to the budding yeast nucleus (23). To fully exploit fission yeast as a system to further our understanding of spindle checkpoint function, we made use of Mad3-GFP to carry out a cytological analysis of the localization of Mad3p. We found Mad3-GFP to be readily visible in a normal unperturbed mitosis. Mad3-GFP forms a single bright spot in prometaphase cells that resides immediately adjacent to the unseparated spindle pole bodies (data not shown). Figure 5A shows Mad3-GFP staining in a series of cells representative of stages of mitosis. Mad3-GFP first becomes visible as a bright focus within the nucleus during prometaphase (Fig. 5A, panels a and b). The foci remain visible up to the metaphase-anaphase transition and colocalize with kinetochores (see below), but as the spindle lengthens during anaphase the Mad3-GFP foci are lost (Fig. 5A, panels d, e, and f). By the time the cell has a fully extended spindle Mad3-GFP is rarely detectable at kinetochores. These data are similar to the pattern described for Bub1p, and we cannot rule out the possibility that a small undetectable pool of Mad3-GFP remains associated with kinetochores throughout anaphase as reported for Bub1p (7).

In summary, Mad3p is recruited to kinetochores during every cell cycle, probably during prometaphase when kinetochores have yet to attach to the spindle apparatus. As the sister chromatids begin to segregate, Mad3-GFP is seen toward the spindle ends. By late anaphase, Mad3-GFP is lost from kinetochores.

Mad3-GFP localizes to unattached kinetochores upon spindle checkpoint activation. To localize the Mad3-GFP fusion protein during a checkpoint arrest, we crossed our Mad3-GFP strain into an *nda3-KM311* background and then conducted the following experiment. Cells were grown to mid-log phase at the permissive temperature of 23°C before being shifted to the restrictive temperature of 16°C for a period of 6 h. Cells were then fixed and visualized.

In the cold, these cells are unable to form a functional mitotic spindle and arrest through the spindle checkpoint with highly condensed chromatids. Sister chromatids remain associated, but are free to diffuse away from the other replicated chromosomes. In all cells examined, we observed one or more sets of paired Mad3-GFP spots, which we refer to from here on as "doublets." In some cells, we were able to see six individual dots representing three doublets, and we never observed more that three sets of doublets. These observations are consistent with Mad3-GFP being located at kinetochores with the number of visible doublets being dependent upon the orientation of the cell on the slide. Figure 5B shows a typical example. The cell to the left of the panel contains three Mad3-GFP doublets. In the DAPI channel, we can clearly see the three sister chromatid pairs; the centromeric heterochromatin of one of the sister chromatid pairs appears to show a constriction in chromosome structure in this region (arrowhead). In the merged image, members of each Mad3-GFP doublet are seen on opposing sides of their associated sister chromatid pair. In the case of the sister chromatid pair showing the constriction at the assumed centromeric region, the Mad3-GFP spots are found

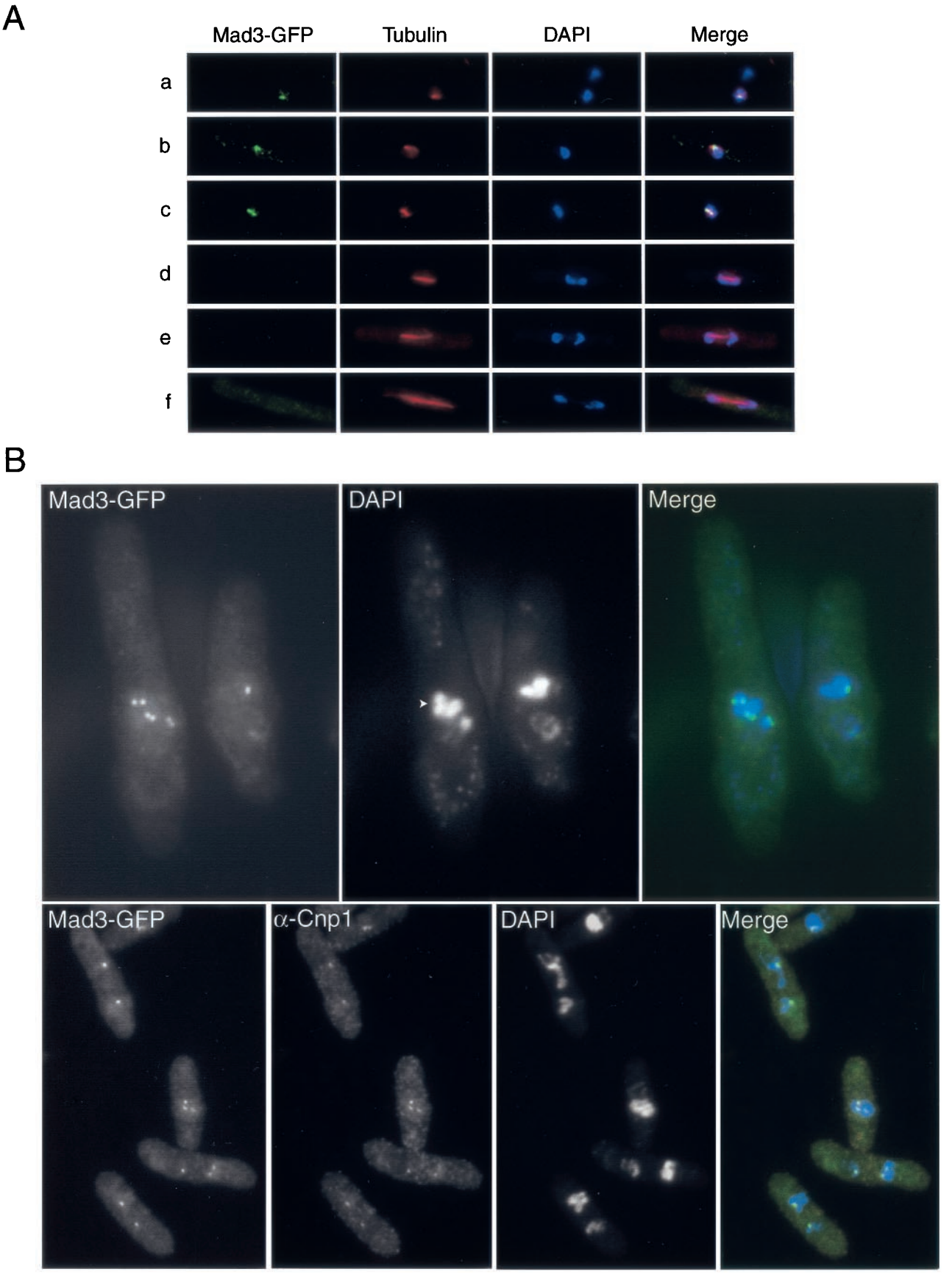
A
Mad3-GFP
Tubulin
DAPI
Merge
a
b
c
d
e
f
B
Mad3-GFP
DAPI
Merge
Mad3-GFP
α-Cnp1
DAPI
Merge

immediately adjacent to the constriction; precisely where kinetochore would be located.

To confirm that these foci were kinetochore structures, we carried out coimmunostaining with antibodies to Cnp1/CENP-A (B. Mellone and R. Allshire, unpublished observations), which is a histone H3 variant specifically incorporated into centromeric chromatin (48). In all *nda3* cells studied, we observed a Mad3-GFP signal colocalizing with the Cnp1/CENP-A signal (Fig. 5B).

Mad3-GFP kinetochore localization is dependent upon the Bub1p kinase, Bub3p, and the Mph1p kinase. With the exception of its Bub3p dependence (53), it is not known in any system whether Mad3/BubR1 recruitment to kinetochores is dependent on other checkpoint components. Therefore we crossed Mad3-GFP into *mad1*Δ, *mad2*Δ, *bub1*Δ, *bub3*Δ, and *mph1*Δ strains. The mutant strains were benomyl sensitive (Fig. 6A), and the Mad3-GFP protein level in these strains was similar to that of wild-type cells, as shown by Western blotting (Fig. 6B).

We then conducted a hydroxyurea (HU) block-and-release experiment with these strains. Log-phase cells were grown in the presence of 11 mM HU for 4 h before being released in to YE5S medium containing 25 μg of CBZ per ml at 23°C. After 2 h of growth, sampling was initiated and then continued at intervals of 15 min. Samples were fixed, processed, and studied by fluorescence microscopy. Both septation and Mad3-GFP localization as a bright nuclear spot were scored.

By 165 min after release from HU, approximately 50% of wild-type cells exhibited Mad3-GFP localized as a single bright nuclear spot. Approximately 20% of *mad1*Δ or *mad2*Δ cells displayed these bright Mad3-GFP spots (Fig. 6C, left panel). Mad3-GFP could clearly form bright foci in the *mad1*Δ and *mad2*Δ backgrounds (Fig. 6D), yet never as often as in the wild type. We attribute this apparent difference to the fact that wild-type cells arrest their cell cycles because of the presence of CBZ in the culture medium, while the *mad*$^-$ mutant cells ignore this, fail to arrest, and pass through mitosis. This point was confirmed in Fig. 6C (right panel), where the number of *mad1*Δ or *mad2*Δ cells septating was seen to be approximately three times that observed for wild-type cells. These Mad3-GFP foci in the *mad1*Δ and *mad2*Δ strains were confirmed to be kinetochores by double labeling with anti-Cnp1/CENPA antibodies (data not shown).

A dramatic difference in Mad3-GFP localization was seen in *bub1*Δ, *bub3*Δ, and *mph1*Δ cells. In these backgrounds, Mad3-GFP was never seen as a bright nuclear spot (Fig. 6C) and was localized diffusely throughout the cell. As expected, the *bub1*Δ, *bub3*Δ, and *mph1*Δ cells also failed to respond to the presence of CBZ and septated (Fig. 6C, right panel). The numerical data presented here represent an average of at least two independent experiments.

In summary, Mad3-GFP is able to localize to kinetochores in *mad1*Δ or *mad2*Δ mutants, but fails to do so in *bub1*Δ, *bub3*Δ, and *mph1*Δ cells. This suggests that the Mph1 and Bub1 protein kinases, as well as the Bub3 protein, are all required for the stable recruitment of Mad3p to kinetochores. On the other hand, while Mad3p forms a stable complex with Mad2p, neither that checkpoint protein nor Mad1p is required for Mad3p kinetochore localization.

DISCUSSION

We have identified the fission yeast *mad3*$^+$gene and found it to be nonessential for normal cell division, but required for spindle checkpoint function. Cells deleted for *mad3*$^+$ are hypersensitive to microtubule poisons such as benomyl, have elevated levels of minichromosome loss rates, and rereplicate their DNA when spindle function is compromised. Furthermore, direct visualization of sister separation events revealed that *mad3*Δ cells precociously separate their sister chromatids when challenged with microtubule poisons. These observations are all indicative of a loss of checkpoint function, and thus we conclude that Mad3p functions as part of the spindle checkpoint.

In addition, we have made two novel and very interesting findings. First, we have shown that Mad3p is required for overexpressed Mad2p to arrest cells in metaphase. Mad1p, Bub1p, and Bub3p are not required for this arrest. Thus, Mad3p appears to have a crucial role in transducing the inhibitory "wait anaphase" signal to the cyclosome or APC. Second, we have shown that Mad3p is recruited to kinetochores in mitosis, and that while Bub1p, Bub3p, and Mph1p functions are required for this localization, Mad1p and Mad2p are not. This provides the first systematic genetic analysis of such kinetochore recruitment for a spindle checkpoint component.

Mad3p and its interactions. We originally identified *mad3*$^+$ by database searching the fission yeast genome sequence data set with protein sequence that is conserved between budding yeast Mad3p and Bub1p. The *mad3*$^+$ ORF does not encode a C-terminal kinase domain, making it more similar to budding yeast *MAD3* than to the vertebrate Bub1/Mad3-related gene coding for BubR1. Fission yeast Mad3p shares 31 and 28% sequence identity across its full length with budding yeast Mad3p and human BubR1, respectively. We confirmed the absence of a C-terminal kinase domain by sequencing the 3′ end of the putative *mad3*$^+$ ORF. Our sequence data were in

FIG. 5. Mad3-GFP localizes to kinetochores early in mitosis. (A) Mad3-GFP localization through a normal unperturbed mitosis. Mad3-GFP (DMSP059) cells were grown to mid-log phase at 23°C before being fixed and processed for immunofluorescence staining. Cells were stained with anti-GFP antibody, antitubulin antibody (TAT1), and DAPI. Mad3-GFP formed a punctate signal in cells that were early in mitosis, containing short spindles (a to c), and this signal was then lost during anaphase. (B) Mad3-GFP is recruited to unattached kinetochores in *nda3KM311*-arrested cells. (Top row) Mad3-GFP *nda3KM311* (DMSP076) cells were grown to mid-log phase at the permissive temperature of 23°C before being shifted down to the restrictive temperature of 16°C for a period of 6 h. Cells were then fixed and visualized by fluorescence microscopy. (Left panel) Mad3-GFP localization to three sets of paired foci. (Middle panel) Individual condensed sister chromatid pairs stained with DAPI. An arrowhead indicates the constriction assumed to be the centromeric region. (Right panel) Merged image revealing that individual Mad3-GFP foci (green) lie on either side of each sister chromatid pair (DNA in blue). (Bottom row) Cells were prepared as described above and costained for Cnp1/CENP-A. Mad3-GFP (green in the merged image) colocalizes with Cnp1/CENP-A (red in the merged image).

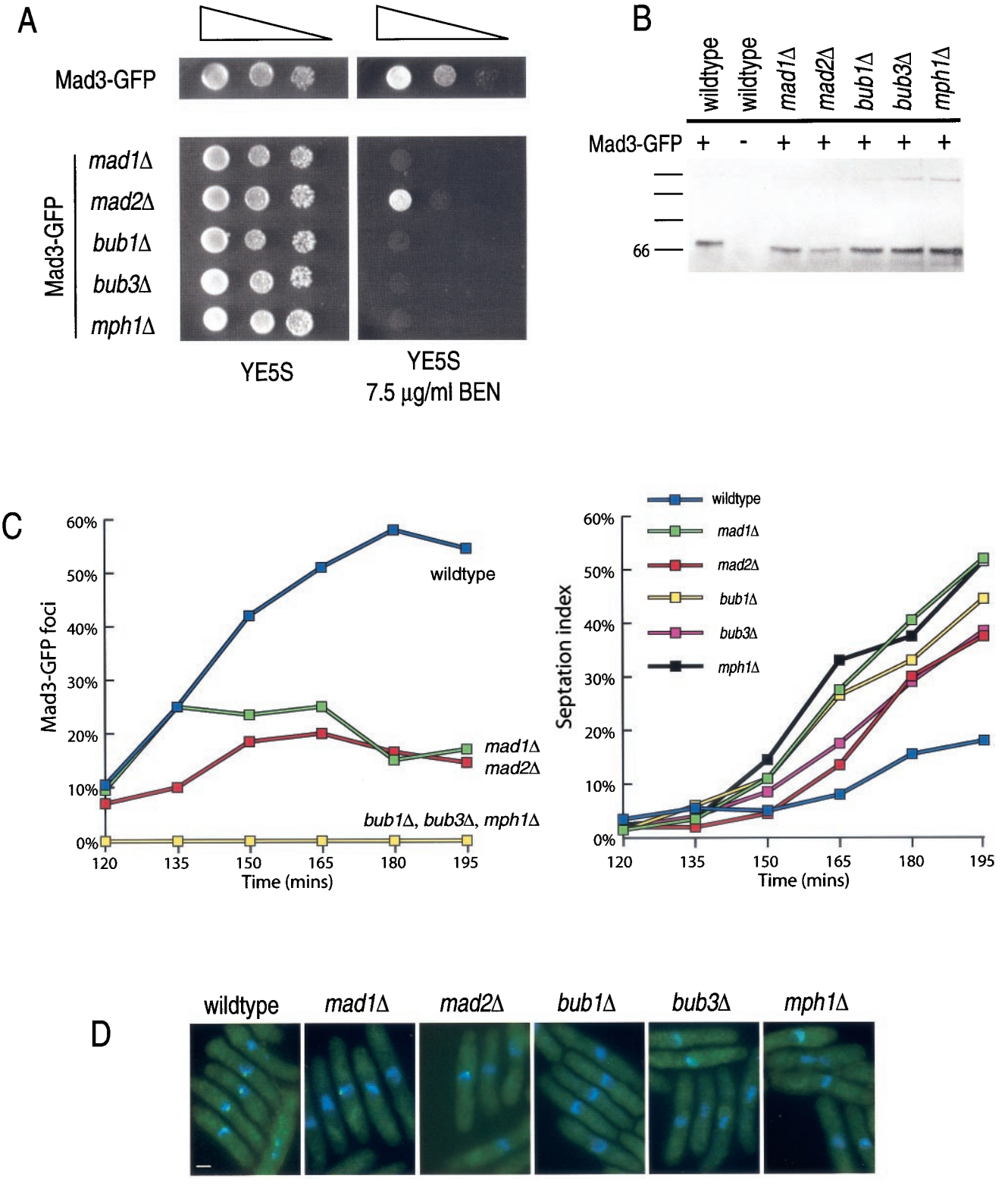

FIG. 6. Stable recruitment of Mad3-GFP to kinetochores is dependent upon Bub1p, Bub3p, and Mph1p. (A) Mad3-GFP (DMSP059) was crossed into cells devoid of individual spindle checkpoint components. Strain construction was confirmed by benomyl sensitivity assay (shown), PCR (data not shown), and Western blotting. (B) Disruption of other spindle checkpoint components does not affect Mad3-GFP expression. Cell lysates were prepared from wild-type (366 line) and Mad3-GFP (DMSP059) cells, as well as spindle checkpoint mutants containing Mad3-GFP (DMSP077, DMSP081, DMSP104, DMSP106, and DMSP134). Lysates were then separated by SDS-PAGE and immunoblotted with antibody specific for GFP. (C) Stable recruitment of Mad3-GFP to kinetochores is dependent upon Bub1p, Bub3p, and Mph1p. Mad3-GFP (DMSP059) and spindle checkpoint mutants containing Mad3-GFP (DMSP077, DMSP081, DMSP104, DMSP106, and DMSP134) were grown to log phase in

complete agreement with that held in the genome data set. Thus, in two divergent yeasts, Mad3p does not have a kinase domain. Interestingly, it has recently been reported that the kinase activity of the human BubR1 kinase is not required for its ability to inhibit the APC in vitro (49). Whether the human protein has evolved to have a second function that is kinase-dependent or the kinase is actually required for BubR1's in vivo checkpoint function remains unclear.

The primary sequence at the C terminus of fission yeast Mad3p does not share obvious homology with budding yeast Mad3p or Bub1p. We have previously shown that this region of the budding yeast protein is sufficient for Bub3p binding (23), which agrees with previous analysis of hBubR1 (53). However, Fig. 4B demonstrates that fission yeast Mad3p does interact with Bub3p, because the two proteins can be coimmunoprecipitated from cell extracts. Perhaps there is structural conservation of the C terminus of Mad3p that cannot be detected by computer-aided alignment of the primary amino acid sequence? Alternatively, a different region of Mad3p may be involved in the Bub3p interaction in fission yeast. Experiments are under way to analyze this interaction in more detail.

When compared with Bub1 proteins, the Mad3 and BubR1 proteins all have an N-terminal extension, which often contains a sequence resembling a KEN box. Such a sequence has been shown to be capable of acting as a Cdh1-dependent APC recognition signal (40). As yet, we have little data suggesting that Mad3p or Bub1p is regulated at the level of proteolysis in fission yeast, although we do generally see an increased level of Mad3p in checkpoint-arrested cells, when compared to asynchronous cultures (Fig. 4A and B), and this is under further investigation. Preliminary experiments, using *cdc25* arrest and release to synchronize cells, show little change in the total levels of Mad3p through the cell cycle. However, it has been reported that the levels of the vertebrate BubR1 protein, as well as its kinase activity, fluctuate with the cell cycle (10).

Fission yeast Mad3p functionally behaves as a homologue of budding yeast Mad3p by acting at the effector end of the checkpoint pathway and coimmunoprecipitating both Mad2p and the Cdc20p homologue Slp1p. Vertebrate BubR1 has also been shown to coimmunoprecipitate $p55^{Cdc20}$ (56) and APC subunits and the kinesin-related motor protein CENP-E (1, 10, 58). Two recent biochemical analyses have highlighted the importance of hBubR1 in a direct inhibition of the APC in vitro (47, 49). In one report, a BubR1/Bub3/Mad2/Cdc20 complex was purified from HeLa cells and found to inhibit mitotic APC 3,000-fold more efficiently than recombinant Mad2p (47). The second report argues that a recombinant hBubR1/Bub3 complex is capable of efficiently inhibiting the APC in an entirely Mad2-independent process (49). Whether hBubR1 and hMad2 complexes function independently or in concert in vivo remains to be seen.

Here we have provided the strongest genetic evidence to date that Mad3p functions at the effector end of the checkpoint pathway. Uniquely among the checkpoint components tested, Mad3p was shown to be required for the arrest observed upon Mad2p overexpression. This shows that Mad3p functions along with, or downstream of, Mad2p to inhibit Slp1/Cdc20p function. This idea is strongly supported at the biochemical level, becauses we have shown that Mad3p binds directly to both of those proteins in fission yeast extracts. Thus, our observations in budding yeast (23) and in fission yeast argue that Mad3p is a second spindle checkpoint component, which along with Mad2p, has a crucial role to play in the in vivo inhibition of the APC. At first glance, these results tend to support the observations of Sudakin et al. (47): both Mad3p and Mad2p are crucial for in vivo checkpoint function, and in fission yeast, the inhibition of the APC observed upon Mad2p overexpression is entirely Mad3p dependent. In neither budding nor fission yeast do we see an obvious cell cycle phenotype upon Mad3p overexpression (unpublished data). Clearly further work will be necessary to determine the precise in vivo roles of the different checkpoint complexes. It is also possible that distinct checkpoint complexes are formed upon different perturbations to microtubule spindles. For example, it has recently been argued that mammalian Mad2 and Bub1/BubR1 recognize distinct spindle attachment and kinetochore tension checkpoints (45), and in maize, it was reported that Mad2 responds to microtubule attachment in mitosis and the absence of tension in meiosis (59). Such conclusions are based on the presence or absence of specific checkpoint proteins at kinetochores under certain conditions. Clearly the non-kinetochore-bound, soluble pools of the checkpoint proteins can also have important functions to play, not least in transmitting the "wait-anaphase signal" from one unattached kinetochore to all of the others in the cell. In yeast, it is now clear that Mad2 is required to respond to a lack of tension in both meiotic and mitotic divisions (41, 46). However, it remains a possibility that quite distinct inhibitory complexes are present in cells at different times, and great care will have to be taken when building models to explain all of the in vivo behaviors and in vitro activities of different checkpoint components.

Mad3p localization and function. We have demonstrated that the localization of Mad3p in yeast is essentially the same as that described for BubR1 in vertebrates. Mad3p localizes to kinetochores during early mitosis, but is then lost from those structures during anaphase. In a few cases, we observed faint staining of kinetochores at the ends of long anaphase spindles (data not shown). We have analyzed Mad3-GFP levels through the cell cycle by immunoblotting after *cdc25*-mediated G_2 arrest and release (data not shown). There was no indication of regulation of Mad3p abundance, and thus the observed recruitment of Mad3-GFP to kinetochores doesn't simply reflect

liquid YE5S before being synchronized by exposure to HU for 4 h at 30°C. Cells were then washed and returned to YE5S medium containing CBZ (25 μg/ml) at 23°C. Periodically, cultures were sampled and examined by fluorescence microscopy for the presence of Mad3-GFP foci and septum formation. (Left panel) Percentage of cells with Mad3-GFP foci ($n = 100$). (Right panel) Septation index ($n = 100$). The percentage of cells is plotted on the *y* axis against time (minutes) after release from HU on the *x* axis. (D) Photographs taken at the 165-min time point from the experiment described above for panel C. The cells shown are stained with DAPI and contain Mad3-GFP. Mad3-GFP foci are seen in wild-type and *mad1*Δ and *mad2*Δ cells, but never in *bub1*Δ, *bub3*Δ, or *mph1*Δ backgrounds. The Mad3-GFP foci in the *mad1*Δ and *mad2*Δ strains were confirmed to be kinetochores through double labeling with anti-Cnp1p antibodies (not shown).

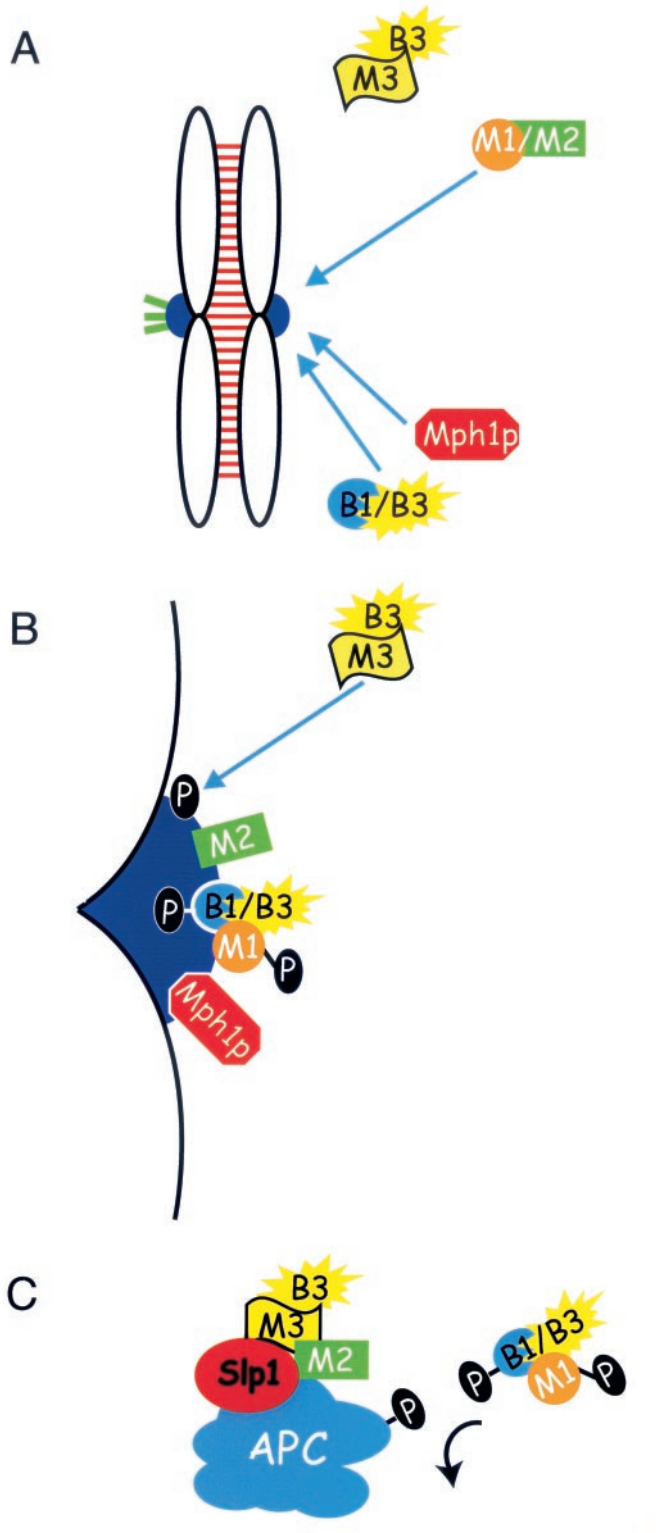

FIG. 7. Model for Mad3p function in the spindle checkpoint. Mad3p functions with Mad2p to inhibit the APC. (A) Unattached kinetochores recruit spindle checkpoint components such as Mph1p, Mad1p/Mad2p, and Bub1p/Bub3p as separate complexes. (B) Once at the kinetochore, Bub1p and Mph1p kinase promote complex rearrangements, yielding a Mad1p/Bub1p/Bub3p complex and free Mad2p. Active Bub1p and/or Mph1p potentially phosphorylates as-yet-unidentified kinetochore components. Mad3p recruitment to the kinetochore then occurs. (C) Mad3p and Mad2p are then released from the kinetochore as a complex to bind Slp1p (NB. this Slp1p could also bind at the kinetochore), thereby inhibiting APC function. APC sensitivity to Mad3p/Mad2p/Slp1p inhibition may be increased through the activity of free Mad1p/Bub1p/Bub3p complex.

the level of the protein. We also observed a very clear localization of Mad3-GFP to the paired kinetochores of sister chromatids during the prolonged checkpoint activation of an *nda3* arrest (Fig. 5B). Similar localization has previously been reported for fission yeast Bub1p (7).

Although most of the spindle checkpoint proteins have been shown to localize to vertebrate kinetochores, the molecular events that occur there remain unclear. It has recently become evident that a rearrangement of Mad/Bub complex constituents occurs upon checkpoint activation, and it seems likely that such rearrangements take place at kinetochores. The relationship of these complex reorganizations to the inhibition of the APC remains quite unclear. In budding yeast, Mad1p becomes hyperphosphorylated and associates with Bub1p and Bub3p, and the formation of this complex occurs in a Mad2p- and Mps1p-dependent fashion and is crucial for checkpoint function (8). Mad2p, although required for complex rearrangement, appears not to be a constituent of the Mad1p/Bub1p/Bub3p complex, and Mad3p is neither part of it nor required for its formation. We currently believe that the Mad1p/Bub1p/Bub3p complex has a signaling role, because we have no evidence for a direct interaction between it and either Cdc20 or the APC. However, it remains a distinct possibility that Bub1 directly modifies the APC or an associated regulator (Fig. 7) and that this is at least partly responsible for APC inhibition.

Here we have demonstrated that kinetochore localization of Mad3p is dependent upon Bub1p, Bub3p, and Mph1p. We propose the following model for Mad3p function within the spindle checkpoint response (Fig. 7). We suggest that Mad3p function is necessary at the effector end of the checkpoint pathway and, in a yet undetermined way, aids Mad2p-mediated inhibition of Slp1/APC activity. In this model, unattached kinetochore structures recruit spindle checkpoint components (Fig. 7A). Originally, it was proposed that Mad1p/Mad2p and Bub1p/Bub3p are targeted to kinetochores as independent complexes (13, 53). However, it has recently been demonstrated that the recruitment of the Mad1p/Mad2p complex to kinetochores is prevented if either the Bub1 or the Mps1 kinase is immunodepleted from *Xenopus* extracts (2, 44). While the Bub1-depleted extract could be "rescued" with recombinant kinase-dead Bub1 protein, that was not the case for XMps1, the kinase activity of which appears to be crucial for spindle checkpoint function. In our model, once the checkpoint proteins have been recruited to the kinetochores, we suggest that a signaling event involving the activity of the Mph1p kinase occurs and that this promotes a rearrangement of checkpoint complexes resulting in formation of the Mad1p/Bub1p/Bub3p complex observed in budding yeast (8) and vertebrates (42). Mad3p is then recruited to the kinetochore (Fig. 7B). It is possible that Mad3p recruitment occurs as a result of Bub1p/Mph1p kinase activity against structural components of the kinetochore, or perhaps the complex rearrangements described above result in exposure of a Mad3p "landing pad." The molecular nature of this Mad3p interaction remains un-

clear, but in mammalian cells, BubR1 associates in a near stoichiometric manner with the microtubule motor CENP-E (1, 11, 58). We are currently investigating whether a similar situation exists in fission yeast. Once at the kinetochore, Mad3p would be available to bind Mad2p, forming a Mad3p/Mad2p complex, which could then directly inhibit Slp1/APC (Fig. 7C). This model predicts that in fission yeast, Mad3p is loaded onto kinetochores after the other spindle checkpoint complexes, and this is supported by studies with human U2OS osteosarcoma cells in which Bub1 and BubR1 were seen to assemble sequentially onto kinetochores (31).

In conclusion, we have demonstrated that fission yeast Mad3p is recruited to unattached kinetochores during mitosis. This, along with its sequence homology and observed protein-protein interactions with Bub3p, Mad2p, and Slp1/Cdc20p, suggests that it is the functional orthologue of both budding yeast Mad3p and vertebrate BubR1. It is now clear that in all organisms analyzed to date, Mad3p and Mad2p form a key link between the checkpoint signaling pathway and direct inhibition of Slp1/APC activity. A precise molecular understanding of this inhibition awaits structural analysis of checkpoint protein complexes and of Cdc20-APC, further purification and reconstitution of checkpoint complexes enabling their activities to be studied in vitro, and careful in vivo experimentation to complement this and confirm physiological functions.

ACKNOWLEDGMENTS

We are grateful to Tomohiro Matsumoto for providing anti-Slp1 and anti-Mad2 antibodies and *mad1*Δ strains; Barbara Mellone and Robin Allshire for anti-Cnp1 antibody; Alison Pidoux for anti-BiP antibody; Shelley Sazer for *mad2*$^+$ and *mph1*$^+$ plasmids and *mph1*Δ strains; Jean-Paul Javerzat for yeast strains and advice on immunofluorescence protocols; and Robin Allshire, Jeremy Brown, Iain Hagan, Alison Pidoux, and Mitsuhiro Yanagida for yeast strains and/or plasmids. We also thank Alison Pidoux, Jennifer Back, and members of our laboratory for comments on the manuscript, helpful discussion, and ongoing support.

This work was supported by the Wellcome Trust. K.G.H. is a Senior Research Fellow and D.N.M. is a graduate student of the Wellcome Trust.

REFERENCES

1. **Abrieu, A., J. A. Kahana, K. W. Wood, and D. W. Cleveland.** 2000. CENP-E as an essential component of the mitotic checkpoint in vitro. Cell **102:**817–826.
2. **Abrieu, A., L. Magnaghi-Jaulin, J. A. Kahana, M. Peter, A. Castro, S. Vigneron, T. Lorca, D. C. Cleveland, and J. C. Labbe.** 2001. Mps1 is a kinetochore-associated kinase essential for the vertebrate mitotic checkpoint. Cell **106:**83–93.
3. **Alfa, C., P. Fantes, J. Hyams, M. McLeod, and E. Warbrick.** 1993. Experiments with fission yeast. Cold Spring Harbor Laboratory Press, Cold Spring Harbor, N.Y.
4. **Allshire, R. C., J. P. Javerzat, N. J. Redhead, and G. Cranston.** 1994. Position effect variegation at fission yeast centromeres. Cell **76:**157–169.
5. **Altschul, S. F., W. Gish, W. Miller, E. W. Myers, and D. J. Lipman.** 1990. Basic local alignment search tool. J. Mol. Biol. **215:**403–410.
6. **Bahler, J., J. Q. Wu, M. S. Longtime, N. G. Shah, A. McKenzie III, A. B. Steever, A. Wach, P. Philippsen, and J. R. Pringle.** 1998. Heterologous modules for efficient and versatile PCR-based gene targeting in *Schizosaccharomyces pombe*. Yeast **14:**943–951.
7. **Bernard, P., K. Hardwick, and J. P. Javerzat.** 1998. Fission yeast bub1 is a mitotic centromere protein essential for the spindle checkpoint and the preservation of correct ploidy through mitosis. J. Cell Biol. **143:**1775–1787.
8. **Brady, D. M., and K. G. Hardwick.** 2000. Complex formation between Mad1p, Bub1p and Bub3p is crucial for spindle checkpoint function. Curr. Biol. **10:**675–678.
9. **Cahill, D. P., C. Lengauer, J. Yu, G. J. Riggins, J. K. V. Willson, S. D. Markowitz, K. W. Kinzler, and B. Vogelstein.** 1998. Mutations of mitotic checkpoint genes in human cancers. Nature **392:**300–303.
10. **Chan, G. K. T., S. A. Jablonski, V. Sudakin, J. C. Little, and T. J. Yen.** 1999. Human BubR1 is a mitotic checkpoint kinase that monitors CENP-E functions at kinetochores and binds the cyclosome/APC. J. Cell Biol. **146:**941–954.
11. **Chan, G. K. T., B. T. Schaar, and T. J. Yen.** 1998. Characterization of the kinetochore binding domain of CENP-E reveals interactions with the kinetochore proteins CENP-F and hBUBR1. J. Cell Biol. **143:**49–63.
12. **Chen, R.-H., D. M. Brady, D. Smith, A. W. Murray, and K. G. Hardwick.** 1999. The spindle checkpoint of budding yeast depends on a tight complex between the Mad1 and Mad2 proteins. Mol. Biol. Cell **10:**2607–2618.
13. **Chen, R. H., A. Shevchenko, M. Mann, and A. W. Murray.** 1998. Spindle checkpoint protein Xmad1 recruits Xmad2 to unattached kinetochores. J. Cell Biol. **143:**283–295.
14. **Chen, R. H., J. C. Waters, E. D. Salmon, and A. W. Murray.** 1996. Association of spindle assembly checkpoint component XMAD2 with unattached kinetochores. Science **274:**242–246.
15. **Ciosk, R., W. Zachariae, C. Michaelis, A. Shevchenko, M. Mann, and K. Nasmyth.** 1998. An ESP1/PDS1 complex regulates loss of sister chromatid cohesion at the metaphase to anaphase transition in yeast. Cell **93:**1067–1076.
16. **Ekwall, E., J.-P. Javerzat, K. Lorentz, H. Schmidt, G. Cranston, and R. C. Allshire.** 1995. The chromo domain protein Swi6: a key component at fission yeast centromeres. Science **269:**1429–1431.
17. **Fang, G., H. Yu, and M. W. Kirschner.** 1998. The checkpoint protein MAD2 and the mitotic regulator CDC20 form a ternary complex with the anaphase-promoting complex to control anaphase initiation. Genes Dev. **12:**1871–1883.
18. **Farr, K. A., and M. A. Hoyt.** 1998. Bub1p kinase activates the *Saccharomyces cerevisiae* spindle assembly checkpoint. Mol. Cell. Biol. **18:**2738–2747.
19. **Funabiki, H., H. Yamano, K. Kumada, K. Nagao, T. Hunt, and M. Yangida.** 1996. Cut2 proteolysis required for sister-chromatid separation in fission yeast. Nature **381:**438–441.
20. **Gardner, R. D., and D. J. Burke.** 2000. The spindle checkpoint: two transitions, two pathways. Trends Cell Biol. **10:**154–158.
21. **Hagan, I., and M. Yanagida.** 1990. Novel potential mitotic motor protein encoded by the fission yeast cut7+ gene. Nature **347:**563–566.
22. **Hardwick, K. G.** 1998. The spindle checkpoint. Trends Genet. **14:**1–4.
23. **Hardwick, K. G., R. J. Johnston, D. Smith, and A. W. M. Murray.** 2000. *MAD3* encodes a novel component of the spindle checkpoint which interacts with Bub3p, Cdc20p and Mad2p. J. Cell Biol. **148:**871–882.
24. **Hardwick, K. G., and A. W. Murray.** 1995. Mad1p, a phosphoprotein component of the spindle assembly checkpoint in budding yeast. J. Cell Biol. **131:**709–720.
25. **Hardwick, K. G., E. Weiss, F. C. Luca, M. Winey, and A. W. Murray.** 1996. Activation of the budding yeast spindle assembly checkpoint without mitotic spindle disruption. Science **273:**953–956.
26. **He, X., T. E. Patterson, and S. Sazer.** 1997. The *Schizosaccharomyces pombe* spindle checkpoint protein mad2p blocks anaphase and genetically interacts with the anaphase-promoting complex. Proc. Natl. Acad. Sci. USA **94:**7965–7970.
27. **He, X. W., M. H. Jones, M. Winey, and S. Sazer.** 1998. mph1, a member of the Mps1-like family of dual specificity protein kinases, is required for the spindle checkpoint in S. pombe. J. Cell Sci. **111:**1635–1647.
28. **Hiraoka, Y., T. Toda, and M. Yanagida.** 1984. The NDA3 gene of fission yeast encodes beta-tubulin: a cold-sensitive nda3 mutation reversibly blocks spindle formation and chromosome movement in mitosis. Cell **39:**349–358.
29. **Hoyt, M. A., L. Totis, and B. T. Roberts.** 1991. S. cerevisiae genes required for cell cycle arrest in response to loss of microtubule function. Cell **66:**507–517.
30. **Hwang, L. H., L. F. Lau, D. L. Smith, C. A. Mistrot, K. G. Hardwick, E. S. Hwang, A. Amon, and A. W. Murray.** 1998. Budding yeast Cdc20: a target of the spindle checkpoint. Science **279:**1041–1044.
31. **Jablonski, S. A., G. K. T. Chan, C. A. Cooke, W. C. Earnshaw, and T. J. Yen.** 1998. The hBUB1 and hBUBR1 kinases sequentially assemble onto kinetochores during prophase with hBUBR1 concentrating at the kinetochore plates in mitosis. Chromosoma **107:**386–396.
32. **Kallio, M., J. Weinstein, J. R. Daum, D. J. Burke, and G. J. Gorbsky.** 1998. Mammalian p55CDC mediates association of the spindle checkpoint protein Mad2 with the cyclosome/anaphase-promoting complex, and is involved in regulating anaphase onset and late mitotic events. J. Cell Biol. **141:**1393–1406.
33. **Kim, S. H., D. P. Lin, S. Matsumoto, A. Kitazono, and T. Matsumoto.** 1998. Fission yeast Slp1: an effector of the Mad2-dependent spindle checkpoint. Science **279:**1045–1047.
34. **Lee, H., A. H. Trainer, L. S. Friedman, F. C. Thistlethwaite, M. J. Evans, B. A. J. Ponder, and A. R. Venkitaraman.** 1999. Mitotic checkpoint inactivation fosters transformation in cells lacking the breast cancer susceptibility gene, *Brca2*. Mol. Cell **4:**1–10.
35. **Li, R., and A. W. Murray.** 1991. Feedback control of mitosis in budding yeast. Cell **66:**519–531.
36. **Martinez-Exposito, M. J., K. B. Kaplan, J. Copeland, and P. K. Sorger.** 1999.

Retention of the Bub3 checkpoint protein on lagging chromosomes. Proc. Natl. Acad. Sci. USA **96:**8493–8498.
37. **Michel, L. S., V. Liberal, A. Chatterjee, R. Kirchwegger, B. Pasche, W. Gerard, M. Dobles, P. K. Sorger, V. V. Murty, and R. Benezra.** 2001. MAD2 haploinsufficiency causes premature anaphase and chromosome instability in mammalian cells. Nature **409:**355–359.
38. **Moreno, S., A. Klar, and P. Nurse.** 1991. Molecular genetic analysis of fission yeast, Schizosaccharomyces pombe. Methods Enzymol. **194:**795–823.
39. **Nicklas, R. B.** 1997. How cells get the right chromosomes. Science **275:**632–637.
40. **Pfleger, C. M., and M. W. Kirschner.** 2000. The KEN box: an APC recognition signal distinct from the D box targeted by CDH. Genes Dev. **14:**655–665.
41. **Schonn, M. A., R. McCarroll, and A. W. M. Murray.** 2000. Requirement of the spindle checkpoint for proper chromosome segregation in budding yeast mitosis. Science **289:**300–303.
42. **Seeley, T. W., L. Wang, and J. Y. Zhen.** 1999. Phosphorylation of human MAD1 by the BUB1 kinase in vitro. Biochem. Biophys. Res. Commun. **257:**589–595.
43. **Shah, J. V., and D. W. Cleveland.** 2000. Waiting for anaphase: Mad2 and the spindle assembly checkpoint. Cell **103:**997–1000.
44. **Sharp-Baker, H., and R. H. Chen.** 2001. Spindle checkpoint protein Bub1 is required for kinetochore localization of Mad1, Mad2, Bub3, and CENP-E, independently of its kinase activity. J. Cell Biol. **153:**1239–1249.
45. **Skoufias, D. A., P. R. Andreasson, F. B. Lacroix, L. Wilson, and R. L. Margolis.** 2001. Mammalian Mad2 and Bub1/BubR1 recognize distinct spindle-attachment and kinetochore-tension checkpoints. Proc. Natl. Acad. Sci. USA **98:**4492–4497.
46. **Stern, B., and A. W. Murray.** 2001. Lack of tension at kinetochores activates the spindle checkpoint in budding yeast. Curr. Biol. **11:**1462–1467.
47. **Sudakin, V., G. K. T. Chan, and T. J. Yen.** 2001. Checkpoint inhibition 0f the APC/C in HeLa cells is mediated by a complex of BubR1, Bub3, Cdc20, Mad2. J. Cell Biol. **154:**925–936.
48. **Takahashi, K., E. S. Chen, and M. Yanagida.** 2000. Requirement of Mis6 centromere connector for localizing a CENP-A-like protein in fission yeast. Science **288:**2215–2219.
49. **Tang, Z., R. Bharadwaj, B. Li, and H. Yu.** 2001. Mad2-independent inhibition of the APCCdc20 by the mitotic checkpoint protein BubR1. Dev. Cell **1:**227–237.
50. **Tatebe, H., G. Goshima, K. Takeda, T. Nakagawa, K. Kinoshita, and M. Yanagida.** 2001. Fission yeast living mitosis visualized by GFP-tagged gene products. Micron **32:**67–74.
51. **Taylor, S. S.** 1999. Chromosome segregation: dual control ensures fidelity. Curr. Biol. **9:**R562–R564.
52. **Taylor, S. S., and F. McKeon.** 1997. Kinetochore localization of murine Bub1 is required for normal mitotic timing and checkpoint response to spindle damage. Cell **89:**727–735.
53. **Taylor, S. T., E. Ha, and F. McKeon.** 1998. The human homolog of Bub3 is required for kinetochore localization of Bub1 and a human Mad3-like protein kinase. J. Cell Biol. **142:**1–11.
54. **Thompson, J. D., T. J. Gibson, F. Plewniak, F. Jeanmougin, and D. G. Higgins.** 1997. The Clustal_X windows interface: flexible strategies for multiple sequence alignment aided by quality analysis tools. Nucleic Acids Res. **24:**4876–4882.
55. **Uhlmann, F., F. Lottspeich, and K. Nasmyth.** 1999. Sister-chromatid separation at anaphase onset is promoted by cleavage of the cohesin subunit Scc1. Nature **400:**37–42.
56. **Wu, H., Z. Lan, W. Li, S. Wu, J. Weinstein, K. M. Sakamoto, and W. Dai.** 2000. p55CDC/hCDC20 is associated with BUBR1 and may be a downstream target of the spindle checkpoint kinase. Oncogene **19:**4557–4562.
57. **Yamamoto, A., V. Guacci, and D. Koshland.** 1996. Pds1p, an inhibitor of anaphase in budding yeast, plays a critical role in the APC and checkpoint pathway(s). J. Cell Biol. **133:**99–110.
58. **Yao, X., A. Abrieu, Y. Zheng, K. F. Sullivan, and D. W. Cleveland.** 2000. CENP-E forms a link between attachment of spindle microtubules to kinetochores and the mitotic checkpoint. Nat. Cell Biol. **2:**484–491.
59. **Yu, H. G., M. G. Muszynski, and R. K. Dawe.** 1999. The maize homologue of the cell cycle checkpoint protein MAD2 reveals kinetochore substructure and contrasting mitotic and meiotic localization patterns. J. Cell Biol. **145:** 425–435.
60. **Zachariae, W., and K. Nasmyth.** 1999. Whose end is destruction: cell division and the anaphase-promoting complex. Genes Dev. **13:**2039–2058.
61. **Zou, H., T. J. McGarry, T. Bernal, and M. W. Kirschner.** 1999. Identification of a vertebrate sister-chromatid separation inhibitor involved in transformation and tumorigenesis. Science **285:**418–421.